

INTERNATIONAL SOCIETY FOR SOIL MECHANICS AND GEOTECHNICAL ENGINEERING



This paper was downloaded from the Online Library of the International Society for Soil Mechanics and Geotechnical Engineering (ISSMGE). The library is available here:

<https://www.issmge.org/publications/online-library>

This is an open-access database that archives thousands of papers published under the Auspices of the ISSMGE and maintained by the Innovation and Development Committee of ISSMGE.

Simulation of liquefaction of unsaturated sand using porous media theory

Simulation de la liquéfaction d'un sable non saturé à l'aide de la théorie des milieux poreux

R. Uzuoka & M. Kazama
Tohoku University, Sendai, Japan

N. Sento & T. Unno
Nihon University, Koriyama, Japan

ABSTRACT

Numerical simulations of unsaturated soil triaxial tests were performed using the porous media theory and a simplified elasto-plastic constitutive model for sand. In the tests, cyclic shear strain was applied to fine clean sand with the same dry density but with different initial suction under undrained conditions. The zero skeleton stress state (i.e. liquefaction) for unsaturated sand was achieved when both the pore air pressure and the water pressure built up to the initial total pressure. Therefore, it is necessary to consider pore air pressure for the proper simulation of liquefaction of unsaturated sand. In the simulation, three phases with a soil skeleton, pore water, and pore air were considered on the basis of porous media theory. The simplified elasto-plastic constitutive model for the soil skeleton was based on the non-associated flow rule and the nonlinear kinematic hardening rule. The simulations provided a satisfactory reproduction of the triaxial test results in the cases where the initial degree of saturation was higher than about 70%.

RÉSUMÉ

Des simulations numériques d'essais triaxiaux sur sols non saturés ont été effectuées en utilisant la théorie des milieux poreux et un modèle de comportement du sable élasto-plastique. Lors des essais, une déformation de cisaillement cyclique a été appliquée à un sable fin et propre ayant une densité sèche constante mais avec des valeurs différentes pour la succion initiale en conditions non drainées. L'état de contrainte nul du squelette (c'est-à-dire la liquéfaction) du sable non saturé a été obtenu lorsque la pression interstitielle (c'est-à-dire à l'intérieur des pores) de l'air et celle de l'eau atteignent la pression totale initiale. Il est donc nécessaire de considérer la pression interstitielle de l'air pour une simulation correcte de la liquéfaction des sables non saturés. Dans la simulation, les trois phases du système (squelette du sol, eau interstitielle et air interstitielle) sont considérées selon la théorie des milieux poreux. Le modèle de comportement élasto-plastique simplifié du squelette du sol est basé sur la loi d'écoulement non associée et la loi de durcissement cinématique non linéaire. Les simulations ont fourni une reproduction satisfaisante des résultats des essais triaxiaux dans les cas où le degré de saturation initial est supérieur à environ 70%.

Keywords :unsaturated sand, liquefaction, porous media theory, constitutive model, cyclic triaxial test

1 INTRODUCTION

Residential or rural fill and soil structures have been severely damaged during earthquakes. Particularly a fill located on an old valley largely deformed due to liquefaction because the ground water level was high after precipitation. Moreover the capillary zone in the fill composed of soil with high water retention is usually thick; therefore it possibly liquefies during earthquake (Uzuoka et al. 2005).

Cyclic triaxial tests with unsaturated soil have been performed by many researchers (e.g. Yoshimi et al. 1989, Tsukamoto et al. 2002, Selim & Burak 2006). It is well known that the cyclic strength of unsaturated sand is larger than that of saturated sand with the same dry density. Recently liquefaction mechanism of unsaturated soil has been discussed (Okamura & Soga 2006, Unno et al. 2008) and it is suggested that the behavior of pore air plays an important role during liquefaction of unsaturated soil.

Liquefaction analyses of unsaturated ground have been performed using porous media theory (e.g. Meroi & Schrefler 1995). Most liquefaction analyses, however, assumed that pore air pressure was zero and the behavior of pore air was not directly treated. In this study, the behavior of three phases with soil skeleton, pore water and pore air are considered based on porous media theory. Numerical simulations of the unsaturated triaxial tests (Unno et al. 2008) are performed using the porous media theory and simplified elasto-plastic constitutive model for sand. The simplified elasto-plastic constitutive model is based on the non-associated flow rule and nonlinear kinematic hardening rule. The constitutive model is basically same as the

model for saturated sand. The effect of suction is taken into account with skeleton stress. The applicability of the numerical method is discussed through the simulations.

2 CYCLIC TRIAXIAL TESTS OF UNSATURATED SAND

Cyclic triaxial tests which continuously measured pore air and water pressure were performed by co-authors (Unno et al. 2008). The details of the tests were described in the literature (Unno et al. 2008). The specimen was made of Toyoura sand by air pluviation method. The relative densities of the specimens were about 60 %. The degree of water saturation was from 20 % to 100 % by controlling air pressure during the isotropic consolidation process. The physical and stress conditions of the specimens after the consolidation are shown in Table 1. Table 1 shows the only cases for the simulations in this study. The pore water pressure was almost zero after the consolidation and the pore air pressure increased with the decrease in water saturation. The mean skeleton stress (e.g. Gallipoli et al. 2003) as mentioned later was about 20 kPa through all cases.

The cyclic shear was applied to the specimen under undrained air and water conditions. The input axial strain was the sinusoidal wave with multi-step amplitudes whose single amplitudes were 0.2, 0.4, 0.8, 1.2, 1.6, and 2.0 with every ten cycles. The frequency of the sinusoidal wave was 0.005 Hz. This loading rate is slow enough to achieve a stable condition of the air and water pressure in the specimen. The test results are shown later with the simulation results.

Table 1. Physical and stress conditions in cyclic triaxial tests

| After consolidation | | | | | | |
|----------------------|-------|------|------|------|------|------|
| Case No. | c-1 | c-3 | c-6 | c-7 | c-9 | c-10 |
| Void ratio | 0.74 | 0.74 | 0.73 | 0.74 | 0.72 | 0.74 |
| Water saturation | 100.0 | 94.8 | 64.8 | 51.6 | 20.2 | 0.0 |
| Mean total stress | 20.5 | 21.4 | 24.1 | 23.7 | 30.0 | 20.0 |
| Pore water pressure | 0.0 | 0.0 | 0.0 | 0.0 | 0.0 | - |
| Pore air pressure | 0.0 | 3.2 | 3.9 | 5.3 | 10.9 | - |
| Suction | 0.0 | 3.2 | 3.9 | 5.3 | 10.9 | - |
| Net stress | 20.5 | 18.2 | 20.2 | 18.4 | 19.1 | - |
| Mean skeleton stress | 20.5 | 21.2 | 22.7 | 21.1 | 21.3 | 20.0 |

| After cyclic loading | | | | | | |
|----------------------|-------|------|------|------|------|------|
| Case No. | c-1 | c-3 | c-6 | c-7 | c-9 | c-10 |
| Void ratio | 0.74 | 0.74 | 0.70 | 0.69 | 0.71 | 0.65 |
| Water saturation | 100.0 | 94.6 | 68.6 | 54.8 | 20.6 | 0.0 |

3 NUMERICAL METHOD

3.1 Balance and constitutive equations

Firstly the basic equations are derived based on porous media theory (de Boer 2000, Schrefler 2002). The partial densities of soil skeleton, pore water and air are defined as follows,

$$\begin{aligned}\rho^s &= n^s \rho^{sR} = (1-n) \rho^{sR} \\ \rho^w &= n^w \rho^{wR} = n s^w \rho^{wR} \\ \rho^a &= n^a \rho^{aR} = n s^a \rho^{aR} = n(1-s^w) \rho^{aR}\end{aligned}\quad (1)$$

where ρ^s , ρ^w and ρ^a are the partial densities of soil skeleton, pore water and air phase respectively. ρ^{sR} , ρ^{wR} and ρ^{aR} are the real densities of each phase, n^s , n^w and n^a are the volume fraction of each phase. n is the porosity, s^w is the degree of water saturation and s^a is the degree of air saturation.

Mass balance equation for α phase ($\alpha = s, w, a$) is

$$\frac{D^\alpha \rho^\alpha}{Dt} + \rho^\alpha \operatorname{div} \mathbf{v}^\alpha = 0 \quad (2)$$

where $D^\alpha \square / Dt$ is the material time derivative with respect to α phase, \mathbf{v}^α is the velocity of α phase. The mass exchange among three phases is ignored. The linear momentum balance equation of α phase is

$$\rho^\alpha \frac{D^\alpha \mathbf{v}^\alpha}{Dt} = \operatorname{div} \boldsymbol{\sigma}^\alpha + \rho^\alpha \mathbf{b} + \hat{\mathbf{p}}^\alpha \quad (3)$$

where $\boldsymbol{\sigma}^\alpha$ is the Cauchy stress tensor of α phase, \mathbf{b} is the body force vector, $\hat{\mathbf{p}}^\alpha$ is the interaction vector against other phases. Although $\hat{\mathbf{p}}^\alpha$ is related to the relative velocity between phases, this term is neglected in the simulation of cyclic triaxial tests only considering stable condition in the specimen. Moreover inertia and body force terms are neglected assuming that stress in the specimen is homogeneous. Therefore only boundary conditions are considered in the simulation of cyclic triaxial tests.

Constitutive equations are the followings. The partial Cauchy stress of each phase is defined as

$$\begin{aligned}\boldsymbol{\sigma}^s &= \boldsymbol{\sigma}' - (1-n)(s^w p^w + s^a p^a) \mathbf{I} \\ \boldsymbol{\sigma}^w &= -n s^w p^w \mathbf{I} \\ \boldsymbol{\sigma}^a &= -n s^a p^a \mathbf{I}\end{aligned}\quad (4)$$

where $\boldsymbol{\sigma}'$ is the skeleton stress tensor (e.g. Gallipoli et al. 2003), p^w is the pore water pressure and p^a is the pore air pressure. These pressures are defined as positive in compression. Only the skeleton stress has constitutive relationship with strain of soil skeleton as shown in section 3.3.

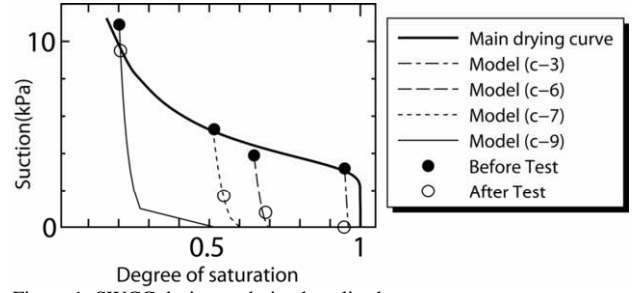


Figure 1. SWCC during undrained cyclic shear

The compressibility of pore water under an isothermal condition is assumed as

$$\frac{D^s \rho^{wR}}{Dt} = \frac{\rho^{wR}}{K^w} \frac{D^s p^w}{Dt} \quad (5)$$

where K^w is the bulk modulus of pore water. The compressibility of pore air under an isothermal condition assumed as

$$\frac{D^s \rho^{aR}}{Dt} = \frac{1}{\Theta \bar{R}} \frac{D^s p^a}{Dt} \quad (6)$$

where Θ is the absolute temperature, \bar{R} is the specific gas constant of air. The constitutive relation between water saturation and suction is assumed as

$$\frac{D^s s^w}{Dt} = c \frac{D^s p^c}{Dt} = c \frac{D^s (p^a - p^w)}{Dt} \quad (7)$$

where c is the specific water capacity. The relationship between suction and water saturation is so called soil water characteristic curve (SWCC).

3.2 SWCC during undrained cyclic shear

Figure 1 shows SWCC from the triaxial tests during undrained cyclic shear. The initial points before the cyclic shear are located on the main drying curve. During undrained cyclic shear, the suction decreases with the increase in the water saturation. Assuming that this process is wetting process, the SWCC during undrained cyclic shear is assumed based on modified VG model (van Genuchten, 1980) as

$$s^w = \beta_{vg} \left\{ 1 + (\alpha_{vg} p^c)^{n_{vg}} \right\}^{-m_{vg}} \quad (8)$$

where the coefficients are assumed as

$$\begin{aligned}\beta_{vg} &= s_0^w \left\{ 1 + (\alpha_{vg} p_0^w)^{n_{vg}} \right\}^{m_{vg}} \\ \alpha_{vg} &= \alpha'_{vg} / s_0^w \\ n_{vg} &= s_0^w \quad m_{vg} = m'_{vg} / s_0^w\end{aligned}\quad (9)$$

where the subscript 0 shows the initial value before cyclic shear. α'_{vg} and m'_{vg} are the material constants. The calibrated results with equations (8) and (9) are shown in Figure 1.

3.3 Simplified constitutive equation for soil skeleton

A simplified constitutive equation for soil skeleton is used in order to discuss the applicability of porous media theory. Assuming that plastic deformation occur only when the deviatoric stress ratio changes, the yield function is assumed as

$$f = \|\boldsymbol{\eta} - \boldsymbol{\alpha}\| - k = \|\mathbf{s} / p' - \boldsymbol{\alpha}\| - k = 0 \quad (10)$$

where $p' = -\text{tr}\boldsymbol{\sigma}'/3$ is the mean skeleton stress, \mathbf{s} is the deviatoric stress tensor of skeleton stress, k is the material parameter which defines the elastic region. $\boldsymbol{\alpha}$ is the kinematic hardening parameter and its nonlinear evolution rule (Armstrong and Frederick 1966) is assumed as

$$\begin{aligned} \dot{\boldsymbol{\alpha}} &= a(b\dot{\mathbf{e}}^p - \boldsymbol{\alpha}\dot{\epsilon}_s^p) \\ \dot{\epsilon}_s^p &= \|\dot{\mathbf{e}}^p\| \end{aligned} \quad (11)$$

where a , b are the material parameters, $\dot{\mathbf{e}}^p$ is the plastic deviatoric strain rate tensor. Assuming non-associated flow rule, the plastic potential function is assumed as

$$g = \|\boldsymbol{\eta} - \boldsymbol{\alpha}\| + M_m \ln(p' / p'_a) = 0 \quad (12)$$

where M_m is the material parameter which defines the critical state ratio, p'_a is p' when $\|\boldsymbol{\eta} - \boldsymbol{\alpha}\| = 0$. Finally the elastic module are assumed as

$$K^e = K^* p' \quad G^e = G^* p' \quad (13)$$

where K^e is the elastic bulk modulus, G^e is the elastic shear modulus, K^* and G^* are the dimensionless elastic module respectively.

3.4 Governing equations for simulation of triaxial test

A right-handed coordinate system is adopted and the z-direction is the vertical axial direction of triaxial specimen. With equations (4) and (7) under the boundary condition that the lateral total stresses are constant, the followings are obtained.

$$\begin{aligned} \dot{\sigma}'_x &= \dot{p}^w (s^w - cp^w + cp^a) + \dot{p}^a (s^a + cp^w - cp^a) = \dot{\sigma}'_y \\ \dot{\sigma}'_z &= \dot{\sigma}'_z + \dot{p}^w (s^w - cp^w + cp^a) + \dot{p}^a (s^a + cp^w - cp^a) \end{aligned} \quad (14)$$

With equations (1), (2), (5), (6) and (7) under undrained conditions for pore water and air, the continuity equations of pore water and air with respect to soil skeleton are obtained as

$$\begin{aligned} n \left(\frac{s^w}{K^w} - c \right) \dot{p}^w + nc\dot{p}^a + s^w \dot{\epsilon}_v^s &= 0 \\ n \left(\frac{s^a}{\rho^{ar} \Theta R} - c \right) \dot{p}^a + nc\dot{p}^w + s^a \dot{\epsilon}_v^s &= 0 \end{aligned} \quad (15)$$

where $\dot{\epsilon}_v^s$ is the volumetric strain rate of soil skeleton. With equations (14) and (15) and with the rate form of constitutive equation of soil skeleton, the unknown variables (the lateral strain rate $\dot{\epsilon}_x^s = \dot{\epsilon}_y^s$, the vertical total stress rate $\dot{\sigma}'_z$, pore water pressure rate \dot{p}^w and pore air pressure rate \dot{p}^a) can be calculated from the input axial strain rate $\dot{\epsilon}_z^s$.

4 NUMERICAL CONDITIONS AND RESULTS

4.1 Calibration of material parameters

The material parameters of constitutive equation of soil skeleton are calibrated with the test results in the cases "c-1" (saturated sand) and "c-10" (dry sand) in Table 1. The constitutive model with the calibrated material parameters reproduced the time histories of void ratio in "c-10" and excess pore water pressure in "c-1" in Figure 2. Table 2 shows the calibrated material

Table 2. Material parameters of constitutive model

| Elasto-plastic model parameters | VG model parameters |
|------------------------------------|--------------------------------------|
| Dimensionless shear modulus, G^* | \square_{vg} |
| Dimensionless bulk modulus, K^* | m_{vg} |
| Nonlinear hardening parameter, a | Physical parameters of water and air |
| Nonlinear hardening parameter, b | K^w (kPa) |
| Critical state stress ratio, M_m | $1/(R(\cdot))$ (s^2/m^2) |
| Yield function parameter, k | \square^{ar} (Mg/m^3) |

*: 1.2 and 0.8 are the values compression and extension side respectively

parameters of the constitutive model. The SWCC parameters in equation (9) were determined to reproduce the change in the water saturation of the specimen during cyclic loading in Figure 1. The SWCC parameters and physical parameters of pore water and air also are shown in Table 2.

4.2 Test and simulation results in unsaturated cases

The time histories of pore water pressure, pore air pressure, suction, mean average skeleton stress and void ratio from tests and simulations in "c-3", "c-6" and "c-7" are shown in Figure 3, 4 and 5 respectively. In the test results (denoted "Test" in the figures), the pore water and air pressure increase during cyclic shear under undrained condition of water and air. In the case "c-3" and "c-6" with higher initial water saturation, the pore water and air pressure attain the mean total stress and the suction becomes almost zero. At the same time the mean skeleton stress also become almost zero and the shear stiffness is lost (Unno et al. 2008). This means that the unsaturated specimen liquefies completely at this time. Although this behavior is similar to liquefaction of saturated sand, the void ratio of unsaturated sand decreases unlike saturated sand. This volumetric change in unsaturated specimen is due to negative dilatancy and high compressibility of pore air. On the other hand, in the case "c-7" with lower initial water saturation, the suction and the mean skeleton stress do not attain zero although the pore water and air pressure increase during cyclic loading.

In the simulated results (denoted "Model" in the figures), the model well reproduces the test results in the case "c-3" and "c-6" with higher initial water saturation. Therefore, the simplified constitutive equation of soil skeleton is applicable to predict liquefaction of unsaturated sand in the framework of three-phase porous media theory. On the other hand, in the case "c-7" with lower initial water saturation, the model overestimates the pore and air pressure of test results. In particular, the error is very large in the case "c-9" (not shown here) and the simplified constitutive is not applicable to this case. The modification of the constitutive equation is necessary in the case with low initial water saturation.

5 CONCLUSIONS

Numerical simulations of the unsaturated triaxial tests were performed using the three-phase porous media theory and simplified elasto-plastic constitutive model for sand. Assuming that undrained cyclic shear process is wetting process, the SWCC during this process is modeled with modified VG model. The simulations well reproduced the triaxial test results in the cases with higher initial degree of saturation than about 70%. The simplified constitutive equation of soil skeleton is applicable to predict liquefaction of unsaturated Toyoura sand in the framework of three-phase porous media theory. The simulation, however, overestimated the pore water and air pressures in the cases with lower initial degree of saturation than about 70%.

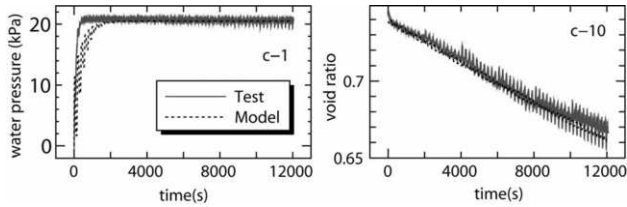


Figure 2. Test and simulation in “c-1” and “c-10”

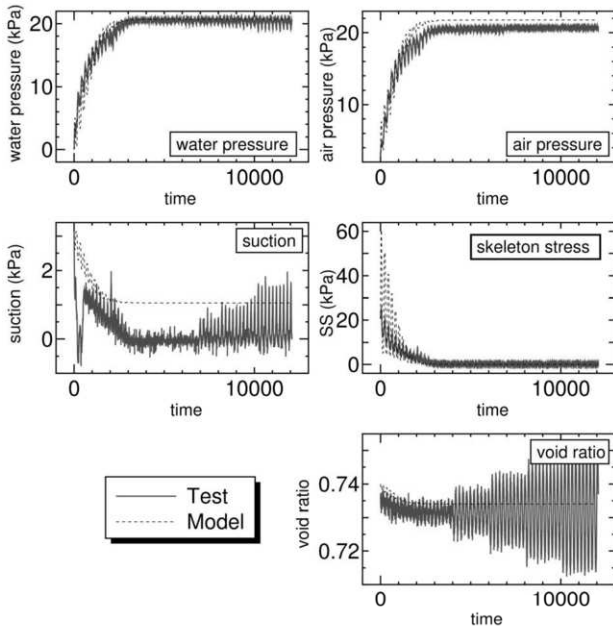


Figure 3. Test and simulation in “c-3”

ACKNOWLEDGEMENT

This study is financially supported by JSPS, Japan Society for the Promotion of Science, for Grants-in-Aid for Scientific Research under Contract No. 17360229. The authors wish to thank to Mr. Tatsuhiro Shoji, formerly graduate student of Tohoku University for his cooperation in the analyses.

REFERENCES

Armstrong, P.J. & Frederick, C.O. 1966. A mathematical representation of the multiaxial Bauschinger effect. C.E.G.B. Report RD/B/N731, Berkeley Nuclear Laboratories, Berkeley, UK.
 de Boer, R. 2000. Contemporary progress in porous media theory. *Applied Mechanics Reviews* 53(12): 323-369.
 Gallipoli, D., Gens, A., Sharma, R. & Vaunat, J. 2003. An elasto-plastic model for unsaturated soil incorporating the effects of suction and degree of saturation on mechanical behaviour. *Geotechnique* 53(1): 123-135.
 van Genuchten, R. 1980. A Closed-form Equation for Predicting the Hydraulic Conductivity of Unsaturated Soils. *Soil Science Society of America Journal* 44: 892-898.
 Meroi, E.A. & Schrefler, B.A. 1995. Large strain static and dynamic semisaturated soil behavior. *Int. J. for Numerical and Analytical Methods in Geomechanics* 19(8): 1-106.
 Okamura, M. & Soga, Y. 2006. Effects of pore fluid compressibility on liquefaction resistance of partially saturated sand. *Soils and Foundations* 46(5): 93-104.
 Schrefler, B.A. 2002. Mechanics and thermodynamics of saturated/unsaturated porous materials and quantitative solutions. *Applied Mechanics Reviews* 55(4): 351-388.

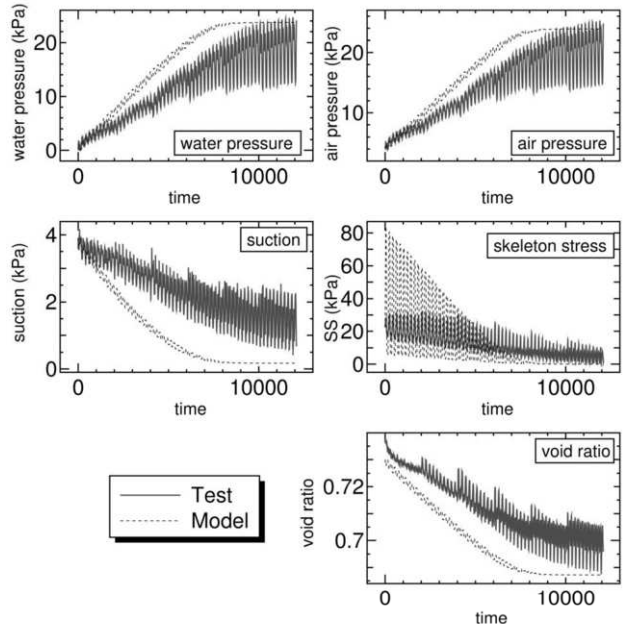


Figure 4. Test and simulation in “c-6”

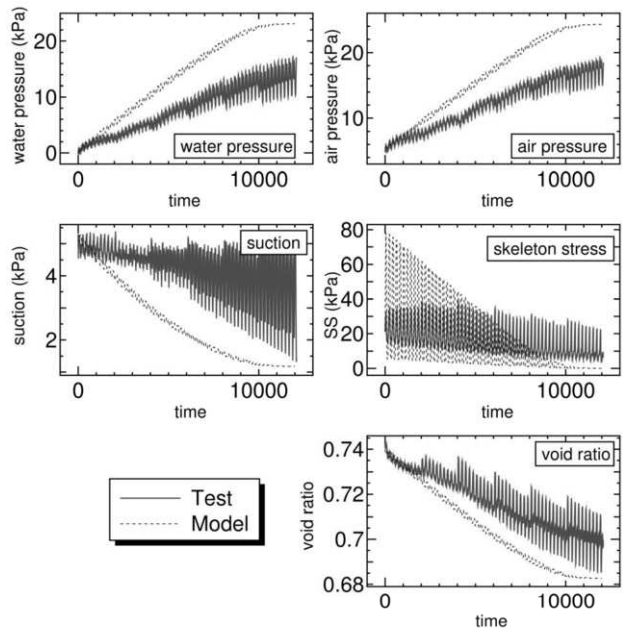


Figure 5. Test and simulation in “c-7”

Selim, A. & Burak, G. 2006. Cyclic stress-strain behavior of partially saturated soils. *Proc. of 3rd Int. Conf. on Unsaturated Soils* 497-507.
 Tsukamoto, Y., Ishihara, K., Nakazawa, H., Kamada, K. & Huang, Y. 2002. Resistance of partly saturated sand to liquefaction with reference to longitudinal and shear wave velocities. *Soils and Foundations* 42(6): 93-104.
 Unno, T., Kazama, M., Uzuoka, R. & Sento, N. 2008. Liquefaction of unsaturated sand considering the pore air pressure and volume compressibility of the soil particle skeleton. *Soils and Foundations* 48(1): 87-99.
 Uzuoka, R., Sento, N., Kazama, M. & Unno, T. 2005. Landslides during the earthquake on May 26 and July 26, 2003 in Miyagi, Japan. *Soils and Foundations* 45(4): 149-163.
 Yoshimi, Y., Tanaka, K. & Tokimatsu, K. 1989. Liquefaction resistance of a partially saturated sand. *Soils and Foundations* 29(3): 157-162.